2014

Quantitative analysis of woodpecker habitat using high-resolution airborne LiDAR estimates of forest structure and composition

James E. Garabedian
North Carolina State University, jegarabe@ncsu.edu

Robert McGaughey
Pacific Northwest Research Station, bmcgaughey@fs.fed.us

Stephen E. Reutebuch
Pacific Northwest Research Station, USDA Forest Service, sreutebuch@fs.fed.us

Bernard R. Parresol
Southern Research Station, USDA Forest Service, bparresol@fs.fed.us

John C. Kilgo
Southern Research Station, USDA Forest Service, jkilgo@fs.fed.us

See next page for additional authors

Remote Sensing of Environment 145 (2014) 68–80

Contents lists available at ScienceDirect

Remote Sensing of Environment

journal homepage: www.elsevier.com/locate/rse

Quantitative analysis of woodpecker habitat using high-resolution airborne LiDAR estimates of forest structure and composition

James E. Garabedian [a,*], Robert J. McGaughey [b], Stephen E. Reutebuch [b], Bernard R. Parresol [c,1], John C. Kilgo [d], Christopher E. Moorman [e], M. Nils Peterson [e]

[a] Department of Forestry and Environmental Resources, North Carolina State University, Box 7646, Raleigh, NC 27695, USA
[b] Pacific Northwest Research Station, USDA Forest Service, University of Washington, PO Box 352100, Seattle, WA 98195-2100, USA
[c] Southern Research Station, USDA Forest Service, Bent Creek Experimental Forest, 1577 Brevard Road, Asheville, NC 28803, USA
[d] Southern Research Station, USDA Forest Service, Savannah River, P.O. Box 700, New Ellenton, SC 29809, USA
[e] Fisheries, Wildlife, and Conservation Biology Program, North Carolina State University, Box 7646, Raleigh, NC 27695, USA

ARTICLE INFO

Article history:
Received 14 August 2013
Received in revised form 6 January 2014
Accepted 28 January 2014
Available online 22 February 2014

Keywords:
Habitat conservation
Forest structure
Landscape
Prediction confidence interval
Red-cockaded woodpecker
Remote sensing
Savannah River Site
Spatially explicit
Wildlife

ABSTRACT

Light detection and ranging (LiDAR) technology has the potential to radically alter the way researchers and managers collect data on wildlife–habitat relationships. To date, the technology has fostered several novel approaches to characterizing avian habitat, but has been limited by the lack of detailed LiDAR-habitat attributes relevant to species across a continuum of spatial grain sizes and habitat requirements. We demonstrate a novel three-step approach for using LiDAR data to evaluate habitat based on multiple habitat attributes and accounting for their influence at multiple grain sizes using federally endangered red-cockaded woodpecker (RCW; *Picoides borealis*) foraging habitat data from the Savannah River Site (SRS) in South Carolina, USA. First, we used high density LiDAR data (10 returns/m^2) to predict detailed forest attributes at 20-m resolution across the entire SRS using a complementary application of nonlinear seemingly unrelated regression and multiple linear regression models. Next, we expanded on previous applications of LiDAR by constructing 95% joint prediction confidence intervals to quantify prediction error at various spatial aggregations and habitat thresholds to determine a biologically and statistically meaningful grain size. Finally, we used aggregations of 20-m cells and associated confidence interval boundaries to demonstrate a new approach to produce maps of RCW foraging habitat conditions based on the guidelines described in the species' recovery plan. Predictive power (R^2) of regression models developed to populate raster layers ranged from 0.34 to 0.81, and prediction error decreased as aggregate size increased, but minimal reductions in prediction error were observed beyond 0.64-ha (4 × 4 20-m cells) aggregates. Mapping habitat quality while accounting for prediction error provided a robust method to determine the potential range of habitat conditions and specific attributes that were limiting in terms of the amount of suitable habitat. The sequential steps of our analytical approach provide a useful framework to extract detailed and reliable habitat attributes for a forest-dwelling habitat specialist, broadening the potential to apply LiDAR in conservation and management of wildlife populations.

1. Introduction

Advances in airborne light detection and ranging (LiDAR) technology have created new potential for ecological research. Over the past decade, technology and analysis methods involving discrete-return, scanning, airborne LiDAR have been applied to quantify various forest attributes (Hyyppä et al., 2008; Næsset, 2004; Zimble et al., 2003). Airborne LiDAR data acquired for forest structure applications typically are collected using a high density of laser pulses (4–10 pulses m^2). Metrics computed from the LiDAR sensor data are used as explanatory variables in predictive models that estimate forest attributes such as basal area (BA), stand height, biomass, and stem volume (Means et al., 2000; Wulder et al., 2012). Characterization of forest structure for areas ranging from a few hundred square meters down to individual trees is possible. The technology has been applied to large areas in several European countries and Canada to conduct forest inventories (Gobakken et al., 2012; Hyyppä et al., 2008; Næsset, 2004), but the potential for the use of LiDAR in ecological studies has yet to be fully realized (García-Feced, Tempel, & Kelly, 2011; Lefsky, Cohen, Parker, & Harding, 2002; Vierling, Vierling, Gould, Martinuzzi, & Clawges, 2008).

* Corresponding author at: Fisheries, Wildlife, and Conservation Biology Program, North Carolina State University, Raleigh, NC 27695, USA. Tel.: +1 9195155578.
E-mail address: jegarabe@ncsu.edu (J.E. Garabedian).
[1] Deceased.

http://dx.doi.org/10.1016/j.rse.2014.01.022
0034-4257/

The accuracy of LiDAR-derived habitat data demonstrated in early forest inventory applications (e.g., Andersen, McGaughey, & Reutebuch, 2005; Leeuwen & Nieuwenhuis, 2010; Lim, Treitz, Wulder, St-Onge, & Flood, 2003) established the foundation for the integration of LiDAR datasets in ecological research. The high-resolution, three-dimensional data generated using LiDAR combined with field observations of wildlife populations provide the opportunity to examine animal–habitat relationships while accounting for the collective effects of fine-grained habitat characteristics, landscape composition, and landscape configuration (Bradbury et al., 2005; Graf, Mathys, & Bollman, 2009; Vierling et al., 2008). LiDAR has been applied in studies of several taxa, including corals (Brock, Wright, Clayton, & Nayegandhi, 2004; Brock, Wright, Kuffner, Hernandez, & Thompson, 2006), fish (Jones, 2006), invertebrates (Müller & Brandl, 2009; Vierling et al., 2011), and small mammals (Nelson, Keller, & Ratnaswamy, 2005). The majority of published studies, however, assess bird–habitat relationships in forests (Vierling et al., 2008). LiDAR data have been applied in these latter studies to investigate reproductive success (Hinsley, Hill, Bellamy, & Balzter, 2006; Hinsley et al., 2008), habitat associations (Clawges, Vierling, Vierling, & Rowell, 2008; Müller, Moning, Bässler, Heurich and Brandl, 2009; Seavy, Viers, & Wood, 2009), species richness (Goetz, Steinberg, Dubayah, & Blair, 2007; Lesak et al., 2011), and community composition (Müller, Stadler and Brandl, 2010).

The predictive power of LiDAR-derived habitat data has fostered novel opportunities to characterize and map avian habitat. In northern Idaho, inclusion of LiDAR-derived data in habitat suitability models produced habitat suitability maps with overall accuracy from 79% to 92% (Martinuzzi et al., 2009). Tattoni, Rizzolli, and Pedrini (2012) reported that LiDAR-derived habitat variables were statistically significant indicators of habitat suitability for three farmland bird species in northeastern Italy, improving predictive power of habitat suitability models and refining the spatial distribution of suitable habitat. Similarly, LiDAR-based habitat suitability models developed for capercaillie (*Tetrao urogallus*) were able to further differentiate and map suitable habitat in a generally suitable forest reserve in the Swiss Pre-Alps (Graf et al., 2009). In New Hampshire, LiDAR-derived habitat variables describing canopy variability were important predictors of black-throated blue warbler (*Dendroica caerulescens*) habitat quality and, in conjunction with LANDSAT variables, could predict site occupancy with up to 90% accuracy (Goetz et al., 2010).

The early successes in studies of avian ecology using LiDAR demonstrate the technology is a viable tool to map habitat quality, but its full potential cannot be reached without new approaches that work for species with narrow niches (Graf et al., 2009; Martinuzzi et al., 2009; Müller et al., 2010). Conventional LiDAR-derived habitat variables (e.g., mean canopy height, canopy cover, foliage height diversity, total vegetation volume) typically used in previous studies may not adequately represent important vegetation characteristics for species with narrow niches. Researchers have noted LiDAR-derived habitat variables may not effectively capture some key habitat characteristics (e.g., differentiate tree species Müller et al., 2009, identify potential RCW cavity trees and hardwood encroachment Smart, Swenson, Christensen, & Sexton, 2012), or meaningful vegetation thresholds (Clawges et al., 2008), thus limiting their predictive power and relevance across different species and ecosystems. Martinuzzi et al. (2009) demonstrated LiDAR can be used to map presence/absence of snags and understory shrubs accurately, but noted the capability of LiDAR to derive continuous estimates of these attributes warrants further study.

Further research is needed to demonstrate the capability to extract accurate and more detailed habitat attributes at various grain sizes relevant to conservation and management (Müller & Brandl, 2009). Determining relationships between scalability and accuracy will also be an important consideration in habitat assessment as these datasets become more widely available, increasing opportunities to apply the technology in ecological studies. Such efforts will facilitate new opportunities to assess habitat quality for multiple species and lead to a broader understanding of local and regional patterns of species occurrence.

We developed a novel approach for using LiDAR data in ecological studies by quantifying habitat conditions across multiple grain sizes and using multiple habitat variables as required to evaluate habitat for species with narrow niches. We used red-cockaded woodpecker (RCW; *Picoides borealis*) foraging habitat quality at the Savannah River Site (SRS) as a model. Red-cockaded woodpecker foraging habitat provides an appropriate model system for evaluating the new methodology because federally endangered RCWs have a narrow niche constrained by multiple variables operating at multiple extents (U.S. Fish & Wildlife Service, 1970; U.S. Fish & Wildlife Service, 2003). The provision of quality foraging habitat is an essential component of RCW recovery. The RCW recovery plan presents two sets of foraging habitat guidelines, one to facilitate population expansion and a second to maintain existing population size. Under the first set, named the recovery standard, foraging habitat quality is evaluated based on the acreage of habitat satisfying specific threshold levels of key structural components including: 1) $\geq$40% herbaceous groundcover; 2) sparse hardwood midstory that is <2.1 m in height; 3) BA and density of pines $\geq$35.6 cm dbh are $\geq$4.6 m^2/ha and $\geq$45 stems/ha, respectively; 4) BA of pines 25.4–35.6 cm dbh is $\leq$9.2 m^2/ha; 5) BA of pines $\geq$25.4 cm dbh is $\geq$2.3 m^2/ha; 6) BA and density of pines <25.4 cm dbh are $\leq$2.3 m^2/ha and $\leq$50 stems/ha, respectively; 7) <30% hardwood overstory; and 8) foraging habitat that satisfies all recommendations of these guidelines (hereafter, foraging habitat guidelines) is not separated by more than 61 m (U.S. Fish & Wildlife Service, 2003). The second set, named the standard for managed stability, recommends each RCW group has access to $\geq$30.4 ha of foraging habitat where BA of pines $\geq$25.4 cm dbh is $\geq$689 m^2 and identifies stands of quality foraging habitat with the following characteristics: 1) $\geq$30 years old; 2) BA of pines $\geq$25.4 cm dbh is between 9.2 and 16.1 m^2/ha; 3) BA of pines <25.4 cm dbh is <4.6 m^2/ha; 4) sparse hardwood midstory that is <2.1 m in height; 5) total BA, including overstory hardwoods, is <18.4 m^2/ha; and 6) stands satisfying these recommendations are not separated by more than 61 m (U.S. Fish & Wildlife Service, 2003). Further, the ability to map detailed foraging habitat attributes over large extents accurately using LiDAR is of substantial importance in the conservation and recovery of the endangered species.

Limited research exists regarding the application of LiDAR to assess RCW foraging habitat. Tweddale et al. (2008) reported canopy pine and hardwoods were classified with 54% and 13% accuracy, respectively. They reported moderate agreement between field- and LiDAR-derived dbh and BA estimates (R^2 of 0.54 and 0.46, respectively). Smart et al. (2012) used low-density discrete-return LiDAR (approximately 0.11 returns/m^2) to compare RCW nesting and foraging habitat and model the species' distribution on the coastal plain of North Carolina. They reported LiDAR-derived maximum tree height, variation of tree heights, and variation in canopy cover could statistically differentiate nesting and foraging habitat. Inclusion of LiDAR-derived habitat variables in RCW distribution models with additional elevation, landcover, and hydrography geospatial variables contributed approximately 28% to model accuracy, but improved predictive success only by 8%. They suggested future analyses of RCW habitat using LiDAR would benefit from extracting additional key structural requirements.

Our objective was to develop and implement a novel approach for using LiDAR to quantify habitat conditions for a forest-dwelling species with a narrow ecological niche. Specifically, we developed an analytical approach to: 1) use LiDAR to model detailed and interrelated forest structural attributes related to RCW foraging habitat quality; 2) analyze the error associated with model predictions at specific threshold values of habitat features and various aggregate sizes to select an appropriate grain size for landscape-scale evaluation of foraging habitat conditions; and 3) apply model predictions at the selected grain size to evaluate RCW foraging habitat conditions at the landscape-scale.

2. Methods

2.1. Study area

The SRS, an 80,267-ha National Environmental Research Park owned and operated by the U.S. Department of Energy (DOE), is located on the Upper Coastal Plain and Sandhills physiographic provinces in South Carolina, USA. The SRS is characterized by sandy soils and gently sloping hills dominated by pines, with hardwoods occurring in riparian areas. Prior to acquisition by DOE in 1951, the majority of SRS uplands were maintained in agricultural fields or had recently been harvested for timber. The U.S. Department of Agriculture (USDA) Forest Service has managed the natural resources of the SRS since 1952 and reforested the majority of the uplands in loblolly (*Pinus taeda*), longleaf (*P. palustris*), and slash (*P. elliottii* var. *elliottii*) pines (Imm & McLeod, 2005). Under intensive management since 1985, the RCW population has grown from 3 groups of 4 birds (Johnston, 2005) to 65 active groups of 246 birds in 2012 (T. Grazia, pers. comm.).

2.2. LiDAR data acquisition and processing

We acquired airborne LiDAR across the SRS in February and March 2009. Data were acquired using two Leica ALS50-II laser scanners mounted in separate fixed-wing aircraft operated during the same time period. Each aircraft collected data for different portions of the SRS (Table 1). The total area covered by the acquisition was approximately 119,000 ha, including approximately 20,000 ha of lands adjacent to SRS. The flight plan consisted of parallel main flights across the site and two cross flights flown perpendicular to the main flight lines. Data were acquired with an average of 10 returns/m^2. At the time of the acquisition, deciduous trees were without foliage. However, several of the broad-leaved species are evergreen or retain dead foliage into the early spring so hardwood species, as a group, are represented by a mix of trees with and without foliage. When computing metrics from LiDAR sensor data (hereafter, LiDAR metrics), we excluded all returns with heights <1 m (relative to the LiDAR-derived ground surface model) to eliminate returns from low-lying grasses and shrubs and to reduce noise due to imperfections in LiDAR ground point filtering. Sensor data were processed using FUSION (McGaughey, 2009). We used a canopy threshold height of 1.5 m when computing total canopy cover. Additional details of the point data reduction and quality assurance analysis are provided by Reutebuch and McGaughey (2012).

2.3. Field measurements

We collected tree measurements on 194 ground calibration plots in the spring of 2009. We used a matrix representing the range of stand height, density, composition, and canopy structure developed with information from the most recent SRS ground inventory conducted in 2000 to select ground calibration plot locations that represented the range of conditions on the SRS. We selected 120 plots in pine forest types, 60 with and 60 without mid-canopy vegetation, 40 plots in mixed pine and hardwood types, and 34 in bottomland hardwoods and baldcypress–tupelo (*Taxodium distichum–Nyssa aquatica*). We recorded plot locations using a dual-frequency, survey-grade GPS receiver (JAVAD Maxor) after tree measurements were completed. At least 600 positions were recorded for each plot center (minimum 10 minute occupation with 1-second epochs). We post-processed position data using a continuously operating reference station (CORS) located close to the study site. We expected plot locations to be accurate to within 1.5 m based on previous experience (Clarkin, 2007; Valbuena, Mauro, Rodriguez-Solano, & Manzanera, 2010).

We used circular, fixed area plots to collect ground calibration vegetation data. The basic plots were 0.04 ha unless fewer than eight dominant or co-dominant trees were present on the plot. For these sparse plots (37% of the plots), we increased plot size to 0.08 ha. On basic plots, measurements for live and dead trees >7.6 cm dbh included species, dbh, height, crown base height, and crown class (i.e., the position of the tree crown relative to the competing vegetation surrounding the tree). We collected the same measurements for trees 2.5–7.6 cm dbh on a 0.004-ha plot nested within the basic plot. Smaller trees on the basic plot but outside the 0.004-ha plot were simply tallied by species and size class (2.5–5.1 cm and 5.1–7.6 cm).

We calculated live, dead, and total BA, tree density (DEN; trees ha^{-1}), mean and median crown length, quadratic mean dbh (QMD), and Lorey's height (BA weighted mean height) for pine, hardwood, and all trees on ground calibration plots (Appendix A). We used BA of pine and hardwood >1.5 m in height and 7.6 cm dbh to estimate canopy composition. For each plot, we computed RCW-specific foraging habitat metrics, including the live BA and DEN of pine trees that were ≥35.6, 25.4–35.6, and 7.6–25.4 cm dbh. We also calculated BA for live hardwoods 7.6–22.9 cm dbh (Table 2; U.S. Fish & Wildlife Service, 2003).

Table 1
Flight parameters and LiDAR sensor settings used to acquire airborne LiDAR on the Savannah River Site between February and March of 2009.

Flying height above ground (planned)	1430 m
Scan angle (flown)	±10°
Scan angle (delivered)[a]	±8°
Average scanning swath width (flown)	505 m
Swath overlap (flown)	62.5%
Maximum returns per pulse	4
Scan frequency	58 Hz
Pulse rate	150 kHz
Beam divergence	0.22 mRad

[a] Returns from the outer 2° of each scan were deleted prior to delivery, which reduced the scan angle, swath width, and overlap.

3. Analytical approach to model forest structure using LiDAR

Our analytical approach involved four sequential steps. First, we quantified the proportion of vegetation without foliage to differentiate between conifer and hardwood vegetation. Next, we used regression methods to relate metrics computed from LiDAR sensor data to forest inventory attributes measured on ground calibration plots. We used the resulting models to predict detailed and interrelated forest structural attributes and subsequently populate raster layers at 20-m resolution with these attributes for all of the SRS. We then quantified the error in model predictions at several *a priori* threshold values, and the change in error as predictions were averaged over several square aggregate sizes (i.e., grain size). Finally, after determining an appropriate aggregate size based on the results of the prediction error analyses, we used the raster layers to assess foraging habitat quality within all non-overlapping foraging partitions (i.e., polygons that equally allocate foraging habitat among individual clusters) of RCW active clusters and recruitment clusters (i.e., clusters of artificial RCW cavities that are not occupied, but maintained to facilitate population expansion) in the entire RCW management area (RCW MA). Accordingly, we present our analysis methods in four parts, corresponding to each of these steps: 1) computing the proportion of vegetation with and without foliage; 2) modeling and mapping forest structure; 3) analyzing the error associated with aggregations of model predictions; and 4) applying model predictions to evaluate RCW foraging habitat.

3.1. Computing the proportion of vegetation without foliage

Because of the importance of hardwood species in the RCW habitat criteria, we wanted to differentiate between conifer and hardwood vegetation using only information derived from the LiDAR data. However, we found that a modeling approach did not provide the desired accuracy. We, therefore, implemented a classification approach to identify the condition of vegetation within 2-m cells. We used a principal component analysis (PCA) to select LiDAR metrics for use in developing

Table 2
Vegetation structural criteria of good quality foraging habitat included in the U.S. Fish and Wildlife Service (2003) recovery standard and managed stability standard along with corresponding criteria codes used in this study.

Criteria code	Foraging habitat recommendation	Source[a]	Calculation of LiDAR-derived habitat variables	Comments
A	Hardwood canopy cover ≤30%	p. 189, #2 (g)	Computed using direct classification of foliage absent/present condition for 2- by 2-m cells and summarized for 20- by 20-m cells	Fraction without foliage includes snags, if present
B	Basal area of pine trees ≥25.4 cm dbh is ≥9.2 and ≤16.1 m^2/ha	p. 293, #3 (b)	Predicted from regression of LiDAR metrics versus BA of pine trees ≥25.4 cm dbh	Upper BA condition ignored, but captured under criteria "G"
C	No hardwood midstory, or if present, sparse and <2.1 m tall.	p. 189, #2 (f)	Calculated a surrogate by subtracting predicted BA of hardwoods ≥22.9 cm dbh from predicted BA of hardwoods ≥7.6 cm dbh	Hardwood mid-canopy vegetation threshold set at ≤1.2 m^2/ha; the majority of hardwoods represented include trees between 7.6 and 15 cm dbh
D	Basal area of pine trees ≥35.6 cm dbh is ≥4.6 m^2/ha and the pines are ≥60 years of age	p. 188, #2 (a)	Predicted from regression of LiDAR metrics versus plot pine BA of trees ≥35.6 cm dbh	Age condition is ignored because most pine stands at SRS are <60 years
E	Density of pine trees ≥35.6 cm dbh is ≥45 trees/ha and the pines are ≥60 years of age	p. 188, #2 (a)	Predicted from regression of LiDAR metrics versus plot pine density of trees ≥35.6 cm dbh	Age condition is ignored because most pine stands at SRS are <60 years
F	Basal area of pine trees <25.4 cm dbh is <2.3 m^2/ha and below 50 stems/ha	p. 188, #2 (c)	Predicted from subtraction of predicted values in cells under criteria "D" from total pine BA regression of LiDAR metrics	Stems/ha condition ignored to simplify analysis and interpretation of method
G	Total stand basal area, including overstory hardwoods, is ≤18.4 m^2/ha[b]	p. 293, #3 (e)	Predicted from regression of LiDAR metrics versus plot BA of trees ≥7.6 cm dbh	

[a] U.S. Fish and Wildlife Service (2003).
[b] The published guidelines (U.S. Fish & Wildlife Service, 2003) incorrectly state 80 ft^2/ac is 23.0 m^2/ha.

classification rules. For the PCA, we computed four types of LiDAR metrics for the 2-m by 2-m cells: 1) metrics computed using the adjusted intensity values for first returns; 2) a pulse penetration metric that quantified the depth to which laser pulses penetrated through the canopy; 3) descriptive statistics computed using the height above ground for LiDAR returns above 2 m; and 4) proportions of first and all returns above height thresholds. For the intensity metrics, we used only the first returns within 2 m of a high-resolution (0.5-m by 0.5-m grid) canopy surface and more than 2 m above the ground. We computed the pulse penetration metric as the difference between the first return surface and a surface created using returns that were the last return of pulses where more than one return was recorded (last of many; Breidenbach, McGaughey, Andersen, Kändler, & Reutebuch, 2007). For the proportions of first and all returns, several height thresholds were used. A basic threshold of 2 m was used to compute a surrogate for canopy cover. We also computed the proportion of first and all returns above the mean height and mode of the height values. The resulting 58 metrics (29 intensity, 19 height, 9 proportions, and penetration) were used in the PCA.

We evaluated the PCA results to select the number of significant components that explained a specified portion of the variability in the data. We then examined variable loadings for each component to select metrics to develop the classification rules. We used the random forest (Breiman, 2001; Liaw & Wiener, 2002) package in R (accessed via the Rattle interface; Williams, 2009) with the LiDAR metrics selected from the PCA to develop the classification rules. We developed classification rules using 70% of the plot data and used the remaining 30% to evaluate the classification error (the default partitioning in Rattle). We summarized the high-resolution classification results for areas corresponding to each ground calibration plot to develop a continuous fraction without foliage (FWF) metric ranging from 0.0 to 1.0 for use as an explanatory variable in predictive models of forest structure. We also summarized the high-resolution classification data over the entire SRS using 20 m cells for use in assessing RCW habitat using the yaImpute package in R (Crookston & Finley, 2008).

3.2. Modeling and mapping forest structure

We used the best subsets approach in the contributed packaged "leaps" (Lumley, 2009) in the R statistical environment (R Development Core Team, 2012) to select a set of LiDAR explanatory variables based on model fit and residual standard error for each forest structure response variable. We used the variance inflation factor (VIF) statistic to eliminate highly collinear predictor variables (Fox & Monette, 1992). If VIF exceeded 5.0 for a candidate predictor variable, we dropped it from the regression model. We used the MASS package (Venables & Ripley, 2002) in R to select Box-Cox transformations of BA and DEN to reduce non-constant variance and satisfy the assumption of constant variance implicit in linear regression techniques. We used plot-level field data and metrics computed from the LiDAR data in conjunction with the resulting models to create spatially explicit inventory layers for SRS.

We used three modeling steps to generate LiDAR estimates of foraging habitat variables (Table 3). In the first step we used nonlinear seemingly unrelated regression (NSUR) to develop models for live BA and DEN of hardwood (HW), softwood (SW), and all plot trees (HS) ≥7.6 cm dbh. This additive regression approach ensured that for each ground calibration plot the HW and SW regression model estimates summed to the regression model estimate for the total plot (Parresol, 2001). We then applied the NSUR approach to the explanatory variables and their coefficients from these regression models as initial values in a system of three equations (one for HW, one for SW, and HS). We then used the Systemfit package (Henningsen & Hamann, 2007) to simultaneously fit models for the HW, SW, and HS equations.

We developed multiple linear regressions to estimate RCW habitat variables. We used the same model selection and evaluation methods as described in the NSUR approach for these models (i.e., model fit, residual standard error, and VIF). To estimate variables bounded by a lower dbh limit (e.g., BA of pines ≥25.4 cm dbh), we developed an independent multiple regression model for each variable above the specified dbh limit; we did not include trees smaller than the dbh limit in ground calibration plot summaries used as response variables. We estimated variables bounded by an upper and lower dbh limit (e.g., BA of pines 7.6–25.4 cm dbh) by subtracting estimates of two regressions. First, we developed a model using only trees greater than the lower dbh limit. Then, we developed a second model using only trees greater than the upper dbh limit. We computed the predictions for both the upper and lower dbh limit regressions across the entire LiDAR acquisition area at 20 m resolution (cell size corresponds to the 0.04-ha field plot size) using ArcGIS Spatial Analyst Raster Calculator (ESRI, 2011). We subtracted the raster layer containing predictions of the second regression model (upper dbh limit) from the predictions of the first (lower dbh limit) to produce an estimate of the habitat variable value for the trees with dbh bounded by the upper and lower dbh limit.

Estimates for variables bounded by upper and lower dbh limits were not compared to ground calibration plot data.

We used BA of hardwoods ≥7.6 and ≥22.9 cm dbh in lieu of hardwood midstory height because the latter could not be quantified using LiDAR. Midstory and understory conditions are components of RCW foraging habitat quality, but are not necessarily well represented in point-cloud data used to develop predictive models (Maltamo et al., 2005). Vegetation that is present in the upper canopy is well sampled by LiDAR pulses, but fewer samples (returns) are measured for vegetation present at lower levels in the canopy. Many of the hardwood species in southern pine forests are shade tolerant and develop under a pine overstory. In such stands, the majority of crowns associated with hardwood species would not be within 2 m of the upper canopy surface and would not be well represented in point-cloud data. Consequently, midstory and understory requirements described in the revised foraging habitat guidelines could not be modeled or used as criteria. For example, because we were unable to explicitly quantify the hardwood midstory as "sparse and less than 2.1 m in height" (U.S. Fish & Wildlife Service, 2003), a surrogate for hardwood midstory conditions based on BA of hardwoods 7.6–22.9 cm dbh was used. Additionally, we only included the BA and density requirements for pines ≥35.6 cm dbh in our criteria; we ignored age requirements because most pine stands at the SRS are <60 years old.

3.3. Analyzing the error associated with model predictions

We constructed joint prediction confidence intervals for each habitat metric that was directly predicted (i.e., not using subtraction) using multiple linear regression to quantify the precision of model predictions. Construction of joint prediction confidence intervals required two values: 1) the standard errors of the predictions (*se*); and 2) a Working-Hotelling value (*W*). The confidence interval boundary points are obtained from

$$\hat{Y} \pm se(t \text{ or } W)$$

where

$$W = \sqrt{pF(1-\alpha; p, n-p)}$$

is the Working-Hotelling value for confidence bands and *se* is the standard error. A scalar value, known as leverage, must be computed to calculate the standard error and is obtained from

$$l_i = x_i \left(X'X\right)^{-1} x_i'$$

where x_i is the *i*th row of the regression design matrix *X*. We used two types of standard errors: 1) for the predicted mean of y_i (i.e., predicted mean of the population); and 2) for the predicted mean of *m* individuals drawn from the distribution of y_i (i.e., predicted mean of *m* 20-m by 20-m cells), which are calculated as

$$s\left(\hat{Y}_i\right) = \sqrt{l_i s^2}$$

and

$$s\left(\widehat{\bar{Y}}_{i(new)}\right) = \sqrt{l_i s^2 + \frac{s^2}{m}}$$

respectively (Parresol, 1992). We used the standard error for the predicted mean of y_i to construct 95% joint prediction confidence intervals for the predicted mean of criteria B, D, and E at the recommended thresholds designated in the RCW recovery plan (Table 2; U.S. Fish & Wildlife Service, 2003).

Data with high spatial resolution (20 m) presented two problems for our analysis. First, the prediction error for individual cells was high, making it difficult to interpret the raster data layers. Second, individual 20-m by 20-m cells were too small to interpret habitat data for the RCW because assessment and management of foraging habitat occur at larger grain sizes (U.S. Fish & Wildlife Service, 2003). To address these problems, we constructed 95% joint confidence intervals using the standard error for the predicted mean of *m* individuals drawn from the distribution of y_i. We adopted this approach to quantify the prediction error associated with the number of predictions (*m*) included in several sizes of square aggregates (2 by 2 cell aggregates, 3 by 3 cell aggregates, etc.) for specified values (y_i). Our goal was to determine the aggregate size that reduced prediction error while still maintaining a meaningful biological grain size. The number of individuals (*m*, or number of 20-m by 20-m

Table 3
RCW habitat criteria regression model summaries, multiple R^2, and root mean square error (RMSE) for basal area (BA; $ft^2\ ac^{-1}$) and tree density (DEN; trees ac^{-1}).

Forest structure variable[a]	Model[b]	Multiple R^2	RMSE
Bounded by lower dbh limit	Non-linear seemingly unrelated regression		
$BA_{sw7.6}$	$(0.5 * (-3.1284 + 0.3834(ElevMean) + 0.2192(COV1) - 0.2596(FWF \times COV1) + 1)^2$	0.78	25.5
$BA_{hw7.6}$	$(0.3 * (-2.9405 + 11.9156(FWF^{0.5}) + 0.00097(ElevP95 \times COV2) + 1)^{3.33}$	0.77	19.6
$BA_{hs7.6}$	$BA_{hs7.6} = BA_{sw7.6} + BA_{hw7.6}$	0.81	27.4
$DEN_{sw7.6}$	$(0.3 * (9.9069 - 0.3073(ElevP95) + 0.1519(COV1) - 0.2109(FWF \times COV1) + 1)^{3.33}$	0.71	109.9
$DEN_{hw7.6}$	$(0.3 * (-4.7332 + 15.7659(FWF^{0.5}) + 0.1079(COV2) + 1)^{3.33}$	0.34	102.6
$DEN_{hs7.6}$	$DEN_{hs7.6} = DEN_{sw7.6} + DEN_{hw7.6}$	0.66	138.2
	Multiple linear regression		
$BA_{sw25.4}$	$(4.8673 - 3.9039(FWF) - 0.0717(COV1) + 0.0051(COV1 \times ElevP90))^2$	0.74	22.5
$BA_{sw35.6}$	$(-0.7525 + 0.1322(ElevP90) - 0.8517(FWF) + 0.0164(COV1))^3$	0.80	16.9
$BA_{hw22.9}$	$(4.2163 - 3.0823(R1A) + 0.1087(FWF \times ElevP90))^3$	0.61	25.8
$DEN_{sw35.6}$	$(-0.0406 + 0.0897(ElevP90) - 1.0559(FWF) + 0.0144(COV1))^3$	0.70	11.7
Bounded by lower and upper dbh limit	Differencing of regression models		
$BA_{sw7.6–25.4}$	$BA_{sw7.6–25.4} = BA_{sw7.6} - BA_{sw25.4}$	–	–
$BA_{hw7.6–22.9}$	$BA_{hw7.6–22.9} = BA_{hw7.6} - BA_{hw22.9}$	–	–

[a] SW signifies a model to estimate the softwood component; HW signifies a model to estimate the hardwood component; HS signifies a model to estimate the total (hardwood and softwood); dbh limits for each variable are listed as either a single lower limit (e.g., $BA_{sw7.6}$ signifies basal area of all softwood trees ≥7.6 cm dbh), or as lower and upper limits (e.g., $BA_{sw7.6–25.4}$ signifies basal area of all softwoods 7.6–25.4 cm dbh).

[b] ElevMean = mean height above ground of all returns > the 1 m ground cutoff height (m); ElevP90 = 90th percentile heights above ground of all LiDAR returns > the 1 m ground cutoff height (m); ElevP95 = 95th percentile heights above ground of all LiDAR returns > the 1 m ground cutoff height (m); FWF = fraction of plot without foliage determined from 2 m by 2 m classifications of LiDAR data (0–1); COV1 = percent canopy cover computed as first returns > 1.5 m canopy threshold height divided by total number of first returns in plot (0–100); COV2 = percent canopy cover computed as all returns > 1.5 m canopy threshold height divided by total number of 1st returns in plot (0–100); R1A = ratio of first to all returns when only returns > 1 m ground cutoff height are counted (0–1).

cells in an aggregate) was based on square samples containing 1 to 100 predictions (i.e., squares containing 1, 4, 9, 16, 25, 36, 49, 64, 81, and 100 cells). The distributions from which individuals were drawn (y_i) were specific values including low, median, and high predicted values and the recommended threshold levels of criteria B, D, and E (Table 2).

3.4. Applying model predictions to evaluate RCW foraging habitat

We performed landscape analysis in ArcGIS (ESRI, 2011) using the predicted forest vegetation habitat metrics. We masked raster layers for the SRS to exclude roads, power line corridors, facilities, streams, and ponds. Because pine stands less than 30 years of age are rarely used by foraging RCWs, we also excluded all these stands using the existing SRS forest stands polygon layer. Although the RCW recovery plan designates separate thresholds for hardwood over-story in loblolly/slash pine stands and longleaf pine stands, we chose to use the loblolly/slash pine threshold due to the species' dominance in RCW foraging habitat.

Starting with cluster locations, we used Thiessen polygons and a buffer operation to create mutually exclusive (i.e., non-overlapping) foraging partitions for situations where circular partitions of adjacent clusters would otherwise overlap (Lipscomb & Williams, 1996; U.S. Fish & Wildlife Service, 2003). Although the preferred method for assessing RCW foraging habitat is to identify the area within the interior (0.4 km) and exterior (0.8 km) radius of the cluster center separately, we combined both partition distances to simplify the presentation of results. We did not attempt to analyze spatial separation of foraging and non-foraging habitat, which is nominally constrained by the RCW foraging habitat guidelines to be no greater than 61 m between adjacent foraging parcels (U.S. Fish & Wildlife Service, 2003).

To determine the amount of foraging habitat available to active and recruitment RCW clusters that satisfied the requirements of our foraging habitat criteria, we enumerated the aggregated cells at the recommended threshold value and then re-calculated the area available using the 95% joint confidence interval boundary points of the recommended threshold. For a given habitat attribute, this method provided upper and lower bounds on the amount of foraging habitat based on the confidence interval boundary points for each attribute, reflecting the uncertainty in predicted habitat data. Finally, we examined the effect of multiple habitat criteria on the resulting amount of suitable habitat by enumerating the cells that met two or more criteria. For this analysis, we did not compute joint statistical limits, but assumed the distributions were independent (i.e., the probability of a predicted value for one attribute was independent of all others). Because the order of the criteria will affect the outcome, we attempted to apply them in a logical sequence starting with more general and less restrictive criteria and progressing to more specific and more restrictive criteria. To remove the effect of criteria order, we also enumerated the number of criteria met within each cell regardless of the criteria sequence.

4. Results

4.1. Applying the analytical approach to model RCW foraging habitat structure

The sequential steps of our analytical approach are capable of extracting an array of detailed and interrelated habitat attributes required to evaluate habitat quality for the RCW. The classification approach used to compute the proportion of vegetation without foliage provided an estimate of the proportion of hardwood vegetation useful for assessing RCW habitat and for modeling other inventory attributes. The regression methods used to model forest structure with LiDAR decompose broadly defined habitat attributes, including BA and density of all trees ≥7.6 cm dbh, into specific hardwood and softwood components that are determinants of RCW foraging habitat quality. Construction of joint prediction confidence intervals facilitates selection of an appropriate aggregate size (i.e., grain size) by considering the relationship between prediction error and scalability at specific habitat thresholds described in the RCW foraging habitat guidelines. Mapping RCW foraging habitat criteria with consideration of prediction confidence interval boundary points facilitates assessment of habitat quality based on the potential range of conditions. Suitable and unsuitable areas (i.e., areas that satisfy criteria requirements vs. those that fail to do so) can be mapped to examine the spatial arrangement of suitable foraging habitat. These results are easily interpreted and can be directly applied to identify areas in need of restoration (based on one or several criteria) or that are suitable for recruitment clusters.

4.2. Computing the proportion of vegetation without foliage

Evaluation of the PCA results showed that four components explained 72% of the variation in the set of LiDAR metrics. Comparison of the variable loadings for the first four components led us to select the variable with the highest loading as a surrogate for the actual component. The following four variables were used in the foliage present/absent classification: mean return intensity (Int.Mean), 40th percentile height divided by the 95th percentile height (Elev.RP40), proportion of first returns above the mean (First.Above.Mean), and coefficient of L-variation (Int.L.CV). Random Forest proved to be a robust classifier using these four variables. For the foliage absent/present classification, overall error was 5.5% for individual 2-m by 2-m cells. The classification was applied across all of the SRS to produce a 2-m resolution raster that classified each cell as FOLIAGE or NO-FOLIAGE. The 2-m raster was then summarized to a 20-m raster to produce the proportion of each 20-m cell that contained vegetation without foliage (fraction without foliage or FWF ranging from 0.0 to 1.0).

4.3. Modeling and mapping forest structure

All but one of the models selected for estimating RCW foraging habitat criteria included three types of explanatory variables: 1) one variable describing dominant canopy height (ElevMean, ElevP90, or ElevP95); 2) one variable describing canopy cover (COV1, COV2, or R1A); and 3) the LiDAR classification variable that estimates the fraction without foliage of the plot's overstory canopy (FWF; Table 3). The use of a dominant canopy height, a canopy cover, and the fraction without foliage explanatory variables provided robust, parsimonious multivariate models. Although inclusion of more LiDAR metrics produced models with marginally higher R^2 statistics, such models tended to over fit the observed data (often resulting in high VIF values between similar LiDAR explanatory metrics, e.g., 80th percentile height and 90th percentile height). Model R^2 values ranged from 0.70 to 0.80 for softwood models and 0.34 to 0.77 for hardwood models (Table 3). The model for density of hardwood trees ≥7.6 cm dbh ($DEN_{hw7.6}$) did not include a dominant canopy height LiDAR variable and had the poorest fit of all models ($R^2 = 0.34$). Data used to develop multiple linear regressions for estimating RCW foraging habitat criteria B, D, and E reflect a wide range of forest types on the SRS; recommended threshold values of each criteria were on the lower spread of the data (Fig. 1).

4.4. Analyzing the error associated with model predictions

A clear relationship existed between aggregate size and prediction error at the recommended threshold values of RCW foraging habitat criteria B, D, and E. Prediction error at the recommended threshold values was largest with one prediction and decreased as the number of predictions, or square aggregate size, increased (Table 4). Beyond 16 predictions, or 0.64-ha square aggregates, reductions in prediction error of m individual predictions were minimal; prediction error of square aggregates larger than 0.64 ha began to converge on the prediction error of the predicted mean of the population ($\overline{X}$; Table 4). Similar relationships between aggregate size and prediction error occurred

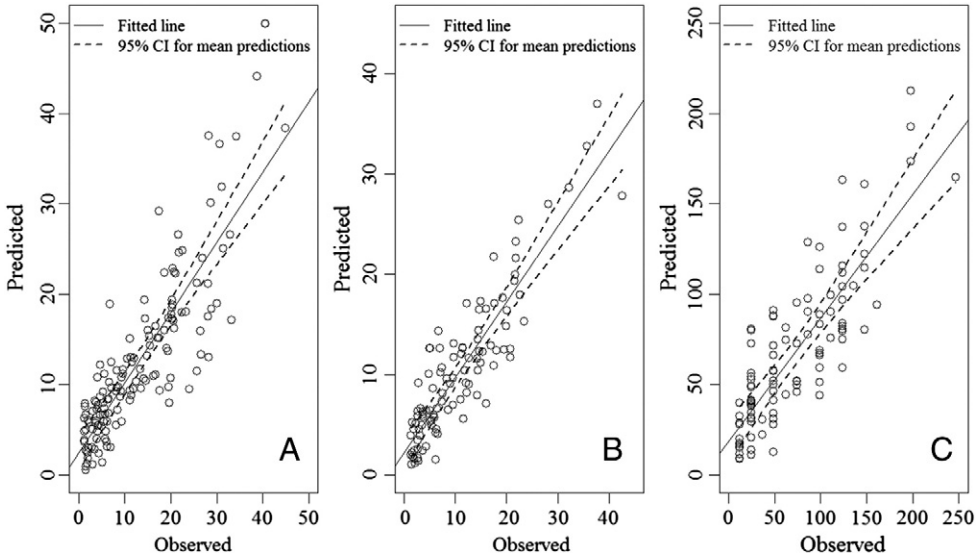

Fig. 1. Scatterplots of field data (Observed) and LiDAR-derived estimates (Predicted) associated with field calibration plots showing fitted lines and 95% confidence bands for the mean predictions of: BA (m^2/ha) of pines ≥25.4 cm dbh (Panel A; criterion B); BA of pines ≥35.6 cm dbh (B; criterion D); and density (trees/ha) of pines ≥35.6 cm dbh (C; criterion E).

at low, median, and high predicted values for criteria B, D, and E (e.g., Fig. 2). As a consequence of sampling error, prediction error at the low and high predicted values of criteria B, D, and E was higher compared to that of the median predicted values (e.g., Fig. 2).

The uncertainty in $\overline{X}$ at RCW foraging habitat criteria threshold values (i.e., mean of y_i) of criteria B and D was approximately ± 2 m^2/ha; uncertainty in $\overline{X}$ at the threshold value of criterion E was approximately ± 14 trees/ha (Table 4). The power transformations used to develop the regression models that generated predictions for each criterion resulted in asymmetrical interval boundary points.

4.5. Applying model predictions to evaluate RCW foraging habitat

Based on the error associated with model predictions, we selected 0.64-ha as the grain size for habitat analyses. There is no previous empirical data to support our selected level of aggregation; however, we believed 0.64-ha was a reasonable size for evaluating habitat attributes by providing more reliable estimates of foraging habitat structure while maintaining a high level of spatial detail in raster layers. We summarized model predictions by the mean of the 16 20-m by 20-m cells that made up each 0.64-ha square aggregate. The amount of foraging habitat satisfying each criterion using the recommended threshold values was similar among all criteria. The total area within RCW foraging partitions that satisfied each criterion ranged from 4431 ha (criterion A) to 3126 ha (criterion E; Table 5). When coupled to the 95% joint prediction confidence interval lower and upper boundary points of model predictions at recommended threshold levels, the amount of potentially suitable foraging habitat for specific criteria (e.g., criteria B or D) varied considerably among non-overlapping RCW foraging partitions (Fig. 3). Due to the range of foraging habitat conditions and sizes of mutually exclusive foraging partitions, certain clusters were allocated less suitable foraging habitat than recommended (e.g., 30.4 ha under the "Managed Stability Standard" or 49 ha under the "Recovery Standard"; U.S. Fish & Wildlife Service, 2003).

In contrast to applying an individual criterion, applying multiple foraging habitat criteria resulted in greater variation in the amount of suitable area among criteria combinations and often decreased area that satisfied the recommended threshold values. The total area within RCW foraging partitions that satisfied the recommended threshold values of multiple criteria applied in sequence ranged from 2926 ha (criteria A and B) to 452 ha (criteria A, B, C, D, F, and G; Table 5). When criteria A, B, and G were applied in sequence as a generalized surrogate for the Managed Stability Standard (i.e., the recommended foraging habitat structure designed to maintain existing population sizes), the total area within RCW foraging partitions that met all three criteria was 1085 ha (Table 5). There were 1782 ha within RCW foraging partitions that did not satisfy the recommended threshold value of any single RCW foraging habitat criterion (Table 6). Regardless of the order criteria were applied, the area within RCW foraging partitions in which the threshold values of multiple criteria were simultaneously satisfied ranged from 1163 ha (area that satisfied any two of the criteria) to 2563 ha (area that satisfied any four of the criteria; Table 6). Approximately 5821 ha of habitat within RCW foraging partitions simultaneously satisfied the requirements of any two to five of the foraging habitat criteria (Table 6).

The spatial arrangement of foraging habitat that satisfied the recommended threshold values of criterion D suggests foraging habitat available to most RCW clusters is fragmented (Fig. 4). When we applied multiple foraging habitat criteria in sequence (e.g., criteria A, B, then G), only a small area of foraging habitat simultaneously satisfied the recommended threshold levels of all three criteria and foraging habitat fragmentation appeared more pronounced (Fig. 5). When we applied multiple foraging habitat criteria in any sequence, the result was a

Table 4
Upper and lower prediction error boundary points at various numbers of aggregated 0.04-ha cells (m) at threshold levels for criteria B (BA [m^2/ha] of pines ≥25.4 cm dbh; predicted threshold = 9.17 m^2/ha), D (BA of pines ≥35.6 cm dbh; predicted threshold = 4.56 m^2/ha), and E (density [trees/ha] of pines ≥35.6 cm dbh; predicted threshold = 45 trees/ha) recommended in the U.S. Fish and Wildlife Service (2003).

	Criterion B (m^2/ha)		Criterion D (m^2/ha)		Criterion E (trees/ha)	
m	Lower	Upper	Lower	Upper	Lower	Upper
1	0.57	28.09	0.41	17.01	4.44	160.40
4	3.49	17.53	1.62	9.83	16.51	93.02
9	4.97	14.63	2.24	8.11	22.66	76.63
16	5.78	13.33	2.57	7.40	25.97	69.74
25	6.27	12.61	2.76	7.03	27.91	66.13
36	6.59	12.16	2.87	6.81	29.14	64.00
49	6.81	11.87	2.95	6.67	29.96	62.64
64	6.97	11.66	3.01	6.58	30.54	61.71
81	7.09	11.51	3.04	6.51	30.95	61.06
100	7.18	11.41	3.07	6.47	31.26	60.58
$\overline{X}$ [a]	7.63	10.84	3.21	6.26	32.69	58.40

[a] Uncertainty in the predicted mean of the population.

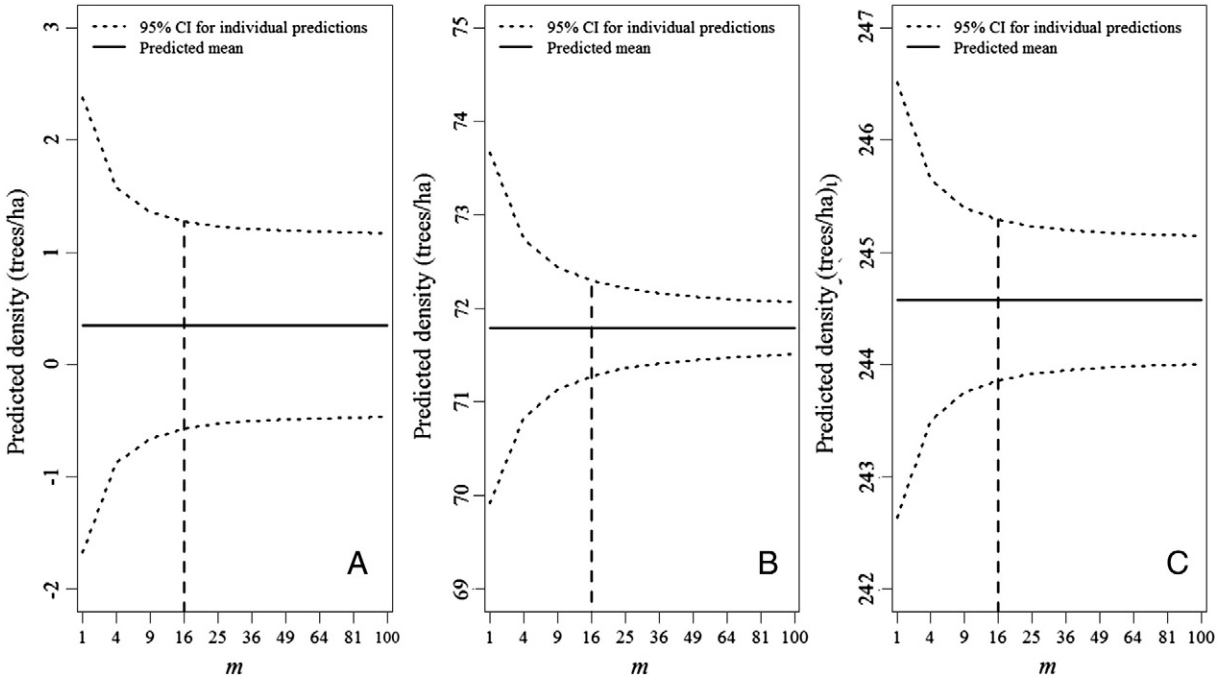

Fig. 2. Relationships between the number of aggregated 0.04 ha cells (m) and prediction error showing the mean predictions and 95% confidence bands for individual estimates at low (0.35 trees/ha), median (71.79 trees/ha), and high (244.57 trees/ha; panels A, B, and C, respectively) predicted values of the density (trees/ha) of pines ≥35.6 cm dbh (criterion E). Vertical lines represent the aggregate cell size selected for habitat analyses.

mosaic of foraging habitat where patches meeting between two and five of the individual foraging habitat criteria appeared to dominate the landscape (Fig. 6).

5. Discussion

The high predictive power of statistical models and reliability of LiDAR-derived habitat data was fostered by sampling a relatively large number of field plots ($n = 194$, or 1 plot/413 ha) across the range of forest conditions at the SRS and obtaining accurate locations for field plots. Without a sufficient sample of forest structure conditions, LiDAR-derived estimates of habitat structure will be less reliable, limiting the value of these data for assessing habitat conditions (Bässler et al., 2011; Hyde et al., 2005). Costs associated with ground calibration plots were low (~10%) relative to the total project cost; thus, we sampled a relatively large number of ground calibration plots to maximize model predictive power and, by extension, prediction reliability. Our models exhibited predictive power comparable to those developed in other studies that sampled field plots at higher densities, including approximately 1 plot/7 ha (Næsset, 2002), 1 plot/43 ha (Tweddale et al., 2008), 1 plot/56 ha (Næsset, 2004). Although we did not conduct a power analysis to determine the number of field plots needed to achieve a desired level of prediction reliability, our results suggest that novel and detailed habitat attributes (e.g., strata-specific estimates of density and BA for pines and hardwoods) can be predicted with reliability comparable to conventional LiDAR-derived habitat attributes with ground calibration plot densities as low as 1 plot/413 ha.. Development of sampling designs that provide coverage of the range of forest conditions or disturbance types (e.g., Helmer et al. 2010) may be more important than the density of ground calibration plots when predicting detailed, wall-to-wall habitat attributes using LiDAR.

Table 5
Total area of RCW management area (RCW MA) and foraging partitions on the SRS meeting single criteria and multiple criteria applied in sequence. Refer to Table 2 for criteria code definitions.

Criteria	RCW MA[a]		RCW foraging partitions[b]	
	Ha	Percent of area	Ha	Percent of area
A	14,536	41	4,431	54
B	14,403	41	3,572	43
C	10,851	31	3,601	44
D	17,122	49	4,158	51
E	13,089	37	3,126	38
F	13,382	38	3,228	39
G	13,262	38	4,054	49
AB	10,646	30	2,926	36
ABC	7,886	22	2,408	29
ABG[c]	3,273	9	1,085	13
ABCD	7,807	22	2,364	29
ABCDF	1,598	5	472	6
ABCDFG	1,409	4	452	6

[a] Total area = 35,269 ha.
[b] Total area of the 72 active and recruitment clusters at the SRS = 8,217 ha.
[c] A generalized surrogate for the Managed Stability Standard (U.S. Fish & Wildlife Service, 2003).

Decomposing broadly defined LiDAR-derived habitat attributes while ensuring additivity of strata-specific predictions is a key component of our analytical approach, allowing researchers to reliably estimate interrelated structural attributes that have direct ecological significance to target species. Our analytical approach serves as a viable model to assess habitat quality for other forest-dwelling wildlife species whose habitat quality is related to a multidimensional framework of structural characteristics. Cerulean warblers (*Dendroica cerulea*) provide an example of such a species because males tend to select territories with dense canopies, high vertical vegetation complexity (i.e., foliage density at specific height strata), and large (e.g., >38 cm dbh), well-spaced trees (Jones & Robertson, 2001; Weakland & Wood, 2005). Hamel (2000) suggested foliage density at specific height strata may be a principal characteristic influencing territory selection, and investigating this relationship using our approach could help clarify habitat requirements for the species.

The trade-offs between prediction reliability and scalability of LiDAR-derived habitat data are easily quantified using our analytical approach, addressing a rarely acknowledged source of uncertainty in LiDAR-derived habitat data applied in ecological studies. A rigorous assessment of prediction error using our methods can be applied to

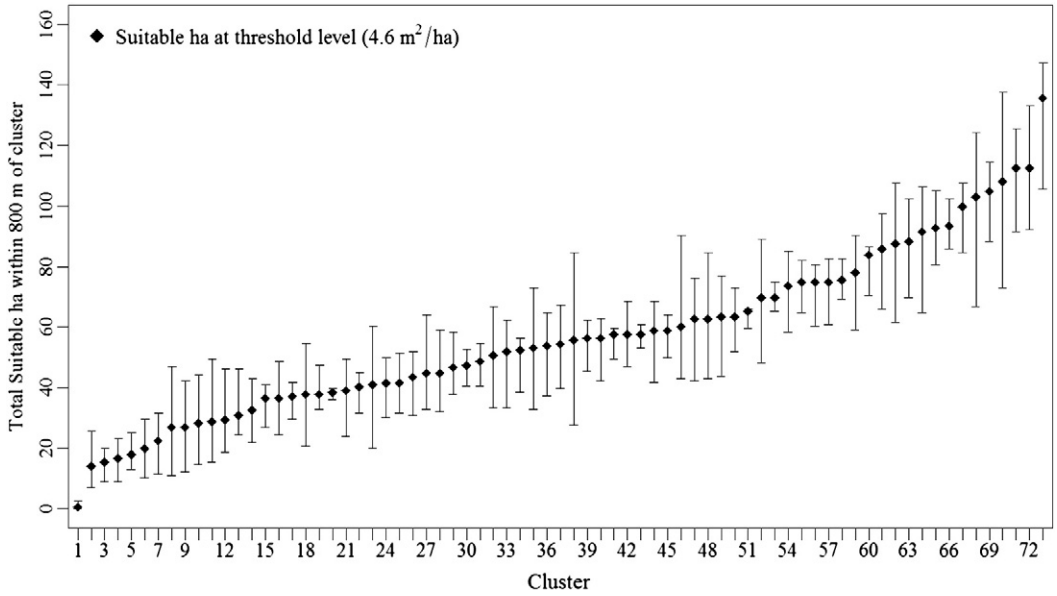

Fig. 3. The amount of foraging habitat at the recommended threshold level for BA (m^2/ha) of pines ≥35.6 cm dbh (criterion D) and 95% joint prediction confidence interval boundary points allocated to non-overlapping RCW active and recruitment clusters (ranked by number of suitable ha) at the Savannah River Site, South Carolina.

sensibly address a critical, but commonly neglected, source of uncertainty that may introduce bias in species-specific investigations of habitat quality using LiDAR-derived habitat data. Aggregation of fine-grained habitat data offers a simple solution to the frequent mismatch between grain sizes of response and predictor variables (e.g., species occurrence and habitat data, respectively), but few studies consider the reliability of newly aggregated habitat data and its influence on predictive models. For instance, northern goshawks (*Accipiter gentilis*) tend to select foraging habitat based on prey availability rather than abundance, the former being largely determined by stand structure (Beier & Drennan, 1997; Greenwald, Crocker-Bedford, Broberg, Suckling, & Tibbitts, 2005). However, because common mammalian prey, such as Abert's squirrel (*Sciurus aberti*), occur at densities of <1 squirrel/ha (Patton, 1984), grain sizes ≥2.25 ha may have greater statistical power to detect patterns in goshawk foraging habitat selection related to stand structure (Beier & Drennan, 1997). Similarly, Graf et al. (2009) used 25-ha aggregates of LiDAR-derived structural variables to support site-specific management initiatives for capercaillie, but noted variables aggregated to grains >25 ha may have improved habitat suitability models because individuals have such large home-range sizes (average of 550 ha; Storch, 1995). Martinuzzi et al. (2009) aggregated 20-m by 20-m cells of LiDAR-derived habitat data to 1 ha as required by the habitat suitability models for four forest-dwelling birds. These studies demonstrate how the appropriate grain size is constrained by a species' natural history, specific hypotheses under examination, and relevant management practices, but a common oversight is the effect of aggregation on habitat data.

Incorporating the relationship between scalability and reliability of LiDAR-derived habitat data is a practical strategy to embrace a source of uncertainty commonly unacknowledged in habitat maps. Considering the relationships between scalability and reliability of LiDAR-derived habitat data as purely a statistical procedure fails to address the impacts of prediction uncertainty on final derived map products. Because LiDAR-based habitat maps have tremendous potential to serve as tools to justify land-use activities and are subject to error, their use should not be based on a single, static representation of the complexities of habitat quality for species with narrow niches. Our results demonstrate uncertainty in LiDAR-derived habitat data influences the spatial distribution and amount of suitable habitat at any grain size, even when models have high predictive power. Visualizing a series of LiDAR-based habitat suitability maps that reflect uncertainty in habitat data provides a more realistic context for management decisions; each map can be interpreted as an alternative, but plausible, environment. For example, northern goshawks select foraging habitat with ≥40% canopy closure (Greenwald et al., 2005), which has been recommended as a minimum threshold in most forests managed for goshawks (Reynolds et al., 1992). Others have suggested goshawk foraging habitat quality can be enhanced with management prescriptions that promote a mosaic of canopy closure conditions that are above the minimum 40%, including >60% canopy closure in >20% of the habitat (Beier & Drennan, 1997).

Table 6
Area in the RCW management area (RCW MA) and within foraging partitions that simultaneously satisfied the requirements of only 0, 1, 2, 3, 4, 5, or 6 foraging habitat criteria.

Maximum number of any criteria satisfied	RCW MA		Foraging partitions	
	Area (ha)	% of total area	Area (ha)	% of total area
0	11,468	32	1782	22
1	636	2	162	2
2	4324	12	1163	14
3	5983	17	1444	18
4	9402	27	2563	31
5	2047	6	651	8
6	1409	4	452	5
	35,269	100	8217[a]	100

[a] Includes both active and recruitment clusters.

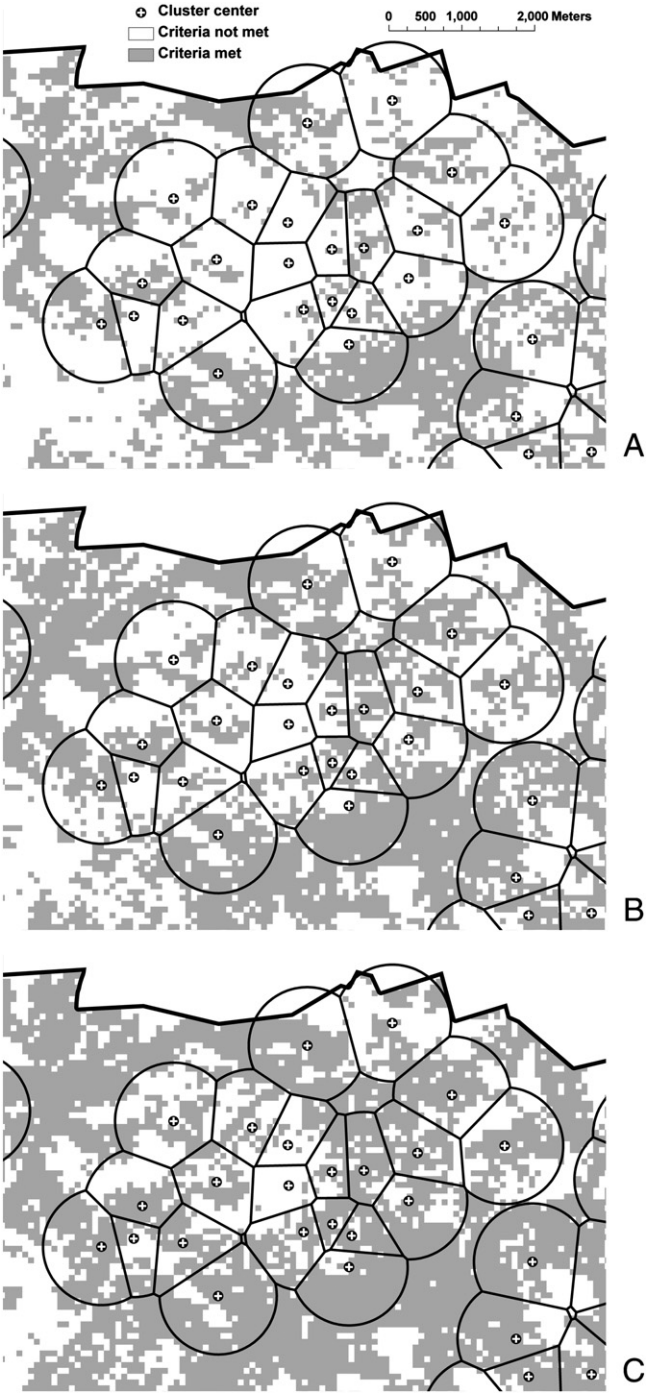

Fig. 4. The spatial arrangement of 0.64-ha aggregates in which the values of the recommended threshold value (panel B) and 95% joint prediction confidence interval boundary points (lower and upper boundary points represented in panels C and A, respectively) for criterion D (BA of pines ≥35.6 cm dbh) were satisfied.

Applying our methods, researchers can produce maps that better illustrate the potential range of habitat conditions, such as spatial configuration of specific canopy closure strata and open areas for a species that prefers large tracts of late-successional forest, across broad extents before initiating management activities.

A valuable application of our approach is the ability to create new opportunities to examine long-standing paradigms of habitat quality for species of conservation concern where consensus on aspects of the species' preferred habitat structure is lacking. Spatially explicit and detailed LiDAR-derived habitat attributes provided new insight into

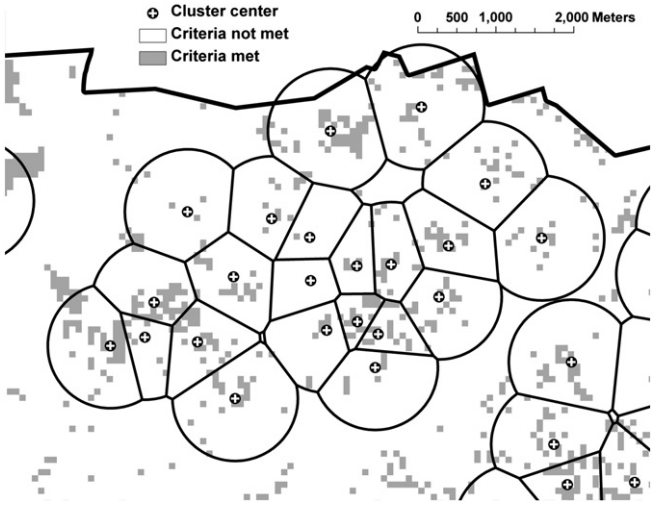

Fig. 5. The spatial arrangement of 0.64-ha aggregates in which the threshold values of criteria A (≤30% hardwood canopy cover), B (BA of pines ≥25.4 cm dbh is ≥9.2 and ≤16.1 m^2/ha), and G (Total BA, including overstory hardwoods, is ≤18.4 m^2/ha) were simultaneously satisfied.

RCW foraging habitat relationships that previously relied on field plot data (e.g., James et al. 1997; Hardesty et al. 1997; James et al. 2001; Walters et al. 2002). Differences in the amount of habitat that satisfied various combinations of criteria allowed us to identify specific habitat attributes that were most restrictive in terms of habitat quality. The results of our study indicate that foraging habitat that does not satisfy all the requirements of the revised foraging habitat guidelines can still support healthy and growing RCW populations; the SRS currently supports 65 active clusters and 246 individuals, a 20% increase from 2011 to 2012. These results suggest our analytical approach using LiDAR can provide new insights into species–habitat relationships where uncertainty persists in the definition of quality habitat. For example, our approach using LiDAR may help validate assumed relationships between northern goshawk reproductive success and the species' preferred foraging habitat structure, which may require habitat data collected over broad extents (Beier, Rogan, Ingraldi, & Rosenstock, 2007). Similarly, our

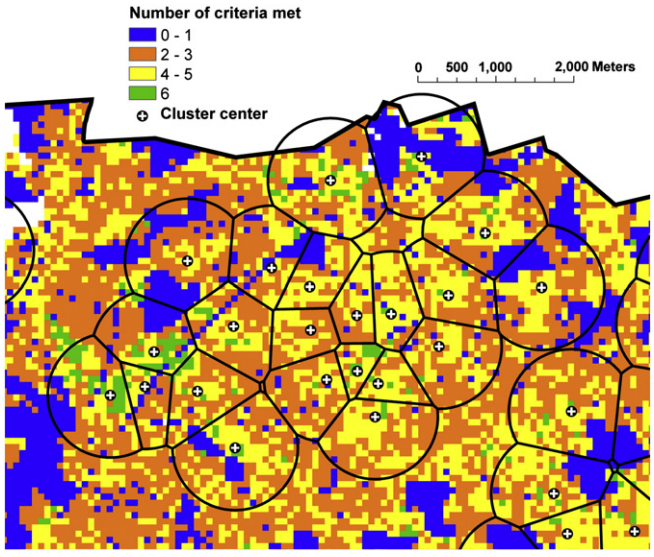

Fig. 6. The spatial arrangement of 0.64-ha aggregates in which the threshold values of only 0, 1, 2, 3, 4, 5, or 6 foraging habitat criteria were simultaneously satisfied.

approach using LiDAR may help substantiate the assumption that intermediate proportions of old-growth forest maximize habitat quality throughout the range of the northern spotted owl (*Strix occidentalis caurina*) by linking fine-grained habitat data collected over broad extents to nest sites and activity centers (Carroll & Johnson, 2008; U.S. Fish & Wildlife Service, 2011). Further, our approach can be applied to expand on other aspects of forest wildlife–habitat relationships, such as linking space-use, reproductive success, or hierarchical habitat selection to vegetation structure (Vierling et al., 2008; Broughton et al. 2012).

In addition to expanding flexibility of LiDAR use in habitat modeling, our approach highlights important factors to consider when collecting LiDAR data. The pine forests of the southeastern USA present several challenges to using LiDAR to quantify wildlife habitat quality. Specifically, over-flight schedules should be chosen based on their relative ability to differentiate canopy cover types in areas where species within the canopy determine wildlife habitat quality. Differentiating predominant cover types in forests that include a mixture of deciduous and non-deciduous hardwoods, pines, and a deciduous conifer (e.g., cypress) can be problematic if LiDAR over-flights are conducted following new foliage development. Characterization of mid- and under-story vegetation is problematic in mixed forests regardless of the time data are collected. Often, there are only a few returns from vegetation in these lower canopy positions. However, differences in the distribution of return heights expressed in the LiDAR-derived metrics seem to capture the presence or absence of this vegetation when height metrics are used to build models. Direct comparisons of field- and LiDAR-derived canopy cover data (e.g., FWF) are difficult because field-derived data do not reflect the spatial arrangement of trees (both horizontal and vertical). Thus, the proportion of canopy without foliage seen from an aerial viewpoint (e.g., LiDAR-derived) may be different from the proportion measured on the ground. We were able to differentiate dominant cover types in a mixed forest by conducting the over-flight in late winter, prior to new foliage development. Field measurements to classify stands or partitions by dominant tree species may still be required, however, until reliable estimates are consistently made based on LiDAR data. Additionally, longleaf pine is of particular importance in terms of RCW habitat quality, and certain foraging habitat guidelines (e.g., criteria A: hardwood canopy cover) are contingent on predominant pine species, yet LiDAR is currently unsuitable for differentiating trees by species. Integrating ancillary remotely sensed habitat data (e.g., multiseason multispectral data) with LiDAR-derived habitat data has the potential to increase accuracy of classifying individual tree species and cover types (Holmgren et al. 2008).

6. Summary

Our analytical approach serves as a promising model in which LiDAR sensor data can be applied in new ways to study habitat relationships of forest-dwelling wildlife that have narrow niches. While our analyses were developed to extract foraging habitat metrics based on the current paradigm of RCW foraging habitat quality, our methods are not restricted to the RCW, the current methods to allocate RCW foraging habitat, or the *a priori* criteria and associated thresholds. LiDAR sensor data can be used to capture more detailed and ecologically meaningful habitat attributes using regression methods that can be tailored to many species with specific or otherwise complex structural habitat requirements. Our methods to assess relationships between scalability and reliability of specific LiDAR-derived habitat attributes provide an additional measure of uncertainty that can be quantified at any grain, promoting grain size selection based on species' natural histories, management practices, and prediction error. Finally, integrating reliability metrics in habitat maps is a simple, but meaningful, technique to represent the potential range of habitat conditions at any grain and extent relevant to a species' natural history and management, allowing land managers to make more informed decisions.

Acknowledgments

We thank the USDA Forest Service-Savannah River staff for operational support and oversight for contract work involved with the acquisition of LiDAR data used in this study. We also thank J. I. Blake for commenting on previous versions of this manuscript. Funding support was provided by U.S. Department of Energy, Savannah River Operations Office through the USDA Forest Service Savannah River (Interagency Agreement DE-AI09-00SR22188) under Cooperative Agreement #SRS 10-CS-11083601-003. We thank A. Poole with the USDA Forest Service-Savannah River for assistance in developing LiDAR raster layers.

Appendix A

A1. Savannah River Site LiDAR ground calibration plot summaries for basal area (BA; m^2 ha^{-1}), tree density (DEN; trees ha^{-1}), and Lorey's height (HT; m). Only live trees were included in these data

Plot metric[a]	*n*	Min	Max	Mean	SD
$BA_{sw7.6}$	194	0.00	80.44	16.92	13.15
$BA_{sw25.4}$	145	1.25	44.86	12.92	9.96
$BA_{sw7.6–25.4}$	151	0.06	80.44	9.33	11.79
$BA_{sw35.6}$	102	1.30	42.55	10.93	8.55
$BA_{hw7.6}$	194	0.00	58.19	6.95	9.40
$BA_{hw22.9}$	84	0.54	51.62	8.80	9.26
$BA_{hw7.6–22.9}$	157	0.10	18.68	3.88	3.77
$BA_{hs7.6}$	194	0.82	97.82	23.86	12.33
$DEN_{sw7.6}$	194	0.00	2741.70	455.49	499.21
$DEN_{sw35.6}$	102	12.35	247.00	71.68	51.77
$DEN_{hw7.6}$	194	0.00	1580.80	288.57	328.86
$DEN_{hs7.6}$	194	24.70	2741.70	744.06	466.71
$HT_{sw7.6}$	179	5.24	37.43	21.18	7.44
$HT_{hw7.6}$	159	6.40	30.87	15.09	5.42
$HT_{hs7.6}$	194	5.47	35.45	20.11	6.55

[a]SW signifies softwood; HW signifies hardwood; HS signifies the total hardwood and softwood component; dbh limits for each variable are listed as either a single lower limit (e.g., $BA_{sw7.6}$ signifies basal area of all softwood trees ≥7.6 cm dbh), or as lower and upper limits (e.g., $BA_{sw7.6–25.4}$ signifies basal area of all softwoods 7.6–25.4 cm dbh.

Appendix B. Supplementary data

Supplementary data associated with this article can be found in the online version, at http://dx.doi.org/10.1016/j.rse.2014.01.022. These data include Google map of the most important areas described in this article.

References

Andersen, H. E., McGaughey, R. J., & Reutebuch, S. E. (2005). Estimating forest canopy fuel parameters using LiDAR data. *Remote Sensing of Environment*, *94*, 441–449.

Bässler, C., Stadler, J., Müller, J., Förster, B., Göttlein, A., & Brandl, R. (2011). LiDAR as a rapid tool to predict forest habitat types in Natura 2000 networks. *Biodiversity and Conservation*, *20*, 465–481.

Beier, P., & Drennan, J. E. (1997). Forest structure and prey abundance in foraging areas of northern goshawks. *Ecological Applications*, *7*, 564–571.

Beier, P., Rogan, E. C., Ingraldi, M. F., & Rosenstock, S. S. (2007). Does forest structure affect reproduction of northern goshawks in ponderosa pine forests? *Journal of Applied Ecology*, *45*, 342–350.

Bradbury, R. B., Hill, R. A., Mason, D. C., Hinsley, S. A., Wilson, J.D., Balzter, H., et al. (2005). Modeling relationships between birds and vegetation structure using airborne LiDAR data: A review with case studies from agricultural and woodland environments. *Ibis*, *147*, 443–452.

Breidenbach, J., McGaughey, R. J., Andersen, H. E., Kändler, G., & Reutebuch, S. E. (2007). A mixed effects model to estimate stand volume by means of small footprint airborne lidar data for an American and German study site. *International Archives of the Photogrammetry, Remote Sensing and Spatial Information Sciences*, *36*, 77–83.

Breiman, L. (2001). Random forests. *Machine Learning*, *45*, 5–32.

Brock, J. C., Wright, C. W., Clayton, T. D., & Nayegandhi, A. (2004). LIDAR optical rugosity of coral reefs in Biscayne National Park, Florida. *Coral Reefs*, *23*, 48–59.

Brock, J. C., Wright, C. W., Kuffner, I. B., Hernandez, R., & Thompson, P. (2006). Airborne lidar sensing of massive stony coral colonies on patch reefs in the northern Florida reef tract. *Remote Sensing of Environment*, *104*, 31–42.

Broughton, R. K., Hill, R. A., Freeman, S. N., Bellamy, P. E., & Hinsley, S. A. (2012). Describing habitat occupation by woodland birds with territory mapping and remotely sensed data: an example using the marsh tit (*Poecile palustris*). *The Condor*, *114*, 812–822.

Carroll, C., & Johnson, D. S. (2008). The importance of being spatial (and reserved): Assessing northern spotted owl habitat relationships with hierarchical Bayesian models. *Conservation Biology*, *22*, 1026–1036.

Clarkin, T. (2007). *Modeling global navigation satellite system positional error under forest canopy based on LIDAR-derived canopy densities.* Thesis, College of Forest Resources, University of Washington, Seattle, WA.

Clawges, R., Vierling, K., Vierling, L., & Rowell, E. (2008). The use of airborne lidar to assess avian species diversity, density, and occurrence in a pine/aspen forest. *Remote Sensing of Environment*, *112*, 2064–2073.

Crookston, N. L., & Finley, A. O. (2008). yaImpute: An R package for kNN imputation. *Journal of Statistical Software*, *23*, 1–16.

ESRI (2011). *ArcGIS (version 9.3).* Redlands: Environmental Systems Research Institute, Inc.

Fox, J., & Monette, G. (1992). Generalized collinearity diagnostics. *Journal of the American Statistical Association*, *87*, 178–183.

García-Feced, C., Tempel, D. J., & Kelly, M. (2011). LiDAR as a tool to characterize wildlife habitat: California spotted owl nesting habitat as an example. *Journal of Forestry*, *109*, 436–443.

Gobakken, T., Næsset, E., Nelson, R., Bollandsås, O. M., Gregoire, T. G., Ståhl, G., et al. (2012). Estimating biomass in Hedmark County, Norway using national forest inventory field plots and airborne laser scanning. *Remote Sensing of Environment*, *123*, 443–456.

Goetz, S. J., Steinberg, D., Betts, M. G., Holmes, R. T., Doran, P. J., Dubayah, R., et al. (2010). Lidar remote sensing variables predict breeding habitat of a Neotropical migrant bird. *Ecology*, *91*, 1569–1576.

Goetz, S., Steinberg, D., Dubayah, R., & Blair, B. (2007). Laser remote sensing of canopy habitat heterogeneity as a predictor of bird species richness in an eastern temperate forest, USA. *Remote Sensing of Environment*, *108*, 254–263.

Graf, R. F., Mathys, L., & Bollman, K. (2009). Habitat assessment for forest dwelling species using LiDAR remote sensing: Capercaillie in the Alps. *Forest Ecology and Management*, *257*, 160–167.

Greenwald, D. N., Crocker-Bedford, D. C., Broberg, L., Suckling, K. F., & Tibbitts, T. (2005). A review of northern goshawk habitat selection in the home range and implications for forest management in the western United States. *Wildlife Society Bulletin*, *33*, 120–128.

Hardesty, J. L., Gault, K. E., & Percival, F. P. (1997). Ecological correlates of red-cockaded woodpecker (Picoides borealis) foraging preference, habitat use, and home range size in northwest Florida (Eglin Air Force Base). *Final Report Research Work Order 99*. University of Florida, Gainesville, Florida: Florida Cooperative Fish and Wildlife Research Unit (137 pp.).

Hamel, P. B. (2000). *Cerulean warbler status assessment.* Minnesota, USA: U.S. Fish and Wildlife Service, Ft. Snelling.

Helmer, E. H., Ruzycki, T. S., Wunderle, J. M., Jr., Vogesser, S., Ruefenacht, B., Kwit, C., Brandeis, T. J., & Ewert, D. N. (2010). Mapping tropical dry forest height, foliage height profiles and disturbance type and age with a time series of cloud-cleared Landsat and ALI image mosaics to characterize avian habitat. *Remote Sensing of Environment*, *114*, 2457–2473.

Henningsen, A., & Hamann, J.D. (2007). systemfit: A package for estimating systems of simultaneous equations in R. *Journal of Statistical Software*, *24*, 1–40.

Hinsley, S. A., Hill, R. A., Bellamy, P. E., & Balzter, H. (2006). The application of lidar in woodland bird ecology: Climate, canopy structure, and habitat quality. *Photogrammetric Engineering and Remote Sensing*, *72*, 1399–1406.

Hinsley, S. A., Hill, R. A., Bellamy, P. E., Harrison, N. M., Speakman, J. R., Wilson, A. K., et al. (2008). Effects of structural and functional habitat gaps on breeding woodland birds: Working harder for less. *Landscape Ecology*, *23*, 615–626.

Holmgren, J., Persson, Å., & Söderman, U. (2008). Species identification of individual trees by combining high resolution LiDAR data with multi-spectral images. *International Journal of Remote Sensing*, *29*, 1537–1552.

Hyde, P., Dubayah, R., Peterson, B., Blair, J. B., Hofton, M., Hunsaker, C., et al. (2005). Mapping forest structure for wildlife habitat analysis using waveform lidar: Validation of montane ecosystems. *Remote Sensing of Environment*, *96*, 427–437.

Hyyppä, J., Hyyppä, H., Leckie, D., Gougeon, F., Yu, X., & Maltamo, M. (2008). Review of methods of small-footprint airborne laser scanning for extracting forest inventory data in boreal forests. *International Journal of Remote Sensing*, *29*, 1339–1366.

Imm, D. W., & McLeod, K. W. (2005). Plant communities. In J. C. Kilgo, & J. I. Blake (Eds.), *Ecology and management of a forested landscape: fifty years of natural resource stewardship on the Savannah River Site* (pp. 106–160). Washington, D. C.: Island Press.

James, F. C., Hess, C. A., & Kufrin, D. (1997). Species-centered environmental analysis: indirect effects of fire history on red-cockaded woodpeckers. *Ecological Applications*, *7*, 118–129.

James, F. C., Hess, C. A., Kicklighter, B. C., & Thum, R. A. (2001). Habitat management and the niche gestalt of the red-cockaded woodpecker in longleaf pine forests. *Ecological Applications*, *11*, 854–870.

Johnston, P. A. (2005). Red-cockaded woodpecker. In J. C. Kilgo, & J. I. Blake (Eds.), *Ecology and management of a forested landscape: Fifty years of natural resource stewardship on the Savannah River Site* (pp. 301–312). Washington, D. C.: Island Press.

Jones, J. L. (2006). Side channel mapping and fish habitat suitability analysis using lidar topography and orthophotography. *Photogrammetric Engineering and Remote Sensing*, *72*, 1202–1206.

Jones, J., & Robertson, R. J. (2001). Territory and nest-site selection of cerulean warblers in eastern Ontario. *The Auk*, *118*, 727–735.

Leeuwen, M., & Nieuwenhuis, M. (2010). Retrieval of forest structural parameters using LiDAR remote sensing. *European Journal of Forest Research*, *129*, 749–770.

Lefsky, M.A., Cohen, W. B., Parker, G. G., & Harding, D. J. (2002). Lidar remote sensing for ecosystem studies. *Bioscience*, *52*, 19–30.

Lesak, A. A., Radeloff, V. C., Hawbaker, T. J., Pidgeon, A.M., Gobakken, T., & Contrucci, K. (2011). Modeling forest songbird species richness using LiDAR-derived measures of forest structure. *Remote Sensing of Environment*, *115*, 2823–2835.

Liaw, A., & Wiener, M. (2002). Classification and regression by Random Forest. *R News*, *2*, 18–22.

Lim, K., Treitz, P., Wulder, M., St-Onge, B., & Flood, M. (2003). LiDAR remote sensing of forest structure. *Progress in Physical Geography*, *27*, 88–106.

Lipscomb, D. J., & Williams, T. M. (1996). A technique for using COV-ARC/INFO GIS to determine red-cockaded woodpecker foraging areas on private lands. *Proceedings of the southern forestry geographic information systems conference* (pp. 255–264). Athens, Georgia, USA: University of Georgia.

Lumley, T. (2009). *Leaps: Regression subset selection (using Fortran code by Alan Miller).* (http://CRAN.R-project.org/package=leaps. Accessed 20 December 2011).

Maltamo, M., Packalén, P., Yu, X., Eerikäinen, K., Hyyppä, J., & Pitkänen, J. (2005). Identifying and quantifying structural characteristics of heterogeneous boreal forests using laser scanning data. *Forest Ecology and Management*, *216*, 41–50.

Martinuzzi, S., Vierling, L. A., Gould, W. A., Falkowski, M. J., Evans, J. S., Hudak, A. T., et al. (2009). Mapping snags and understory shrubs for a LiDAR-based assessment of wildlife habitat suitability. *Remote Sensing of Environment*, *113*, 2533–2546.

McGaughey, R. J. (2009). *FUSION/LDV: software for LIDAR data analysis and visualization, version 2.9.* Pacific Northwest Research Station: U.S. USDA Forest Service.

Means, J. E., Acker, S. A., Brandon, J. F., Renslow, M., Emerson, L., & Hendrix, C. J. (2000). Predicting forest stand characteristics with airborne scanning lidar. *Photogrammetric Engineering and Remote Sensing*, *66*, 1367–1371.

Müller, J., & Brandl, R. (2009). Assessing biodiversity by remote sensing in mountainous terrain: the potential of LiDAR to predict forest beetle assemblages. *Journal of Applied Ecology*, *46*, 897–905.

Müller, J., Moning, C., Bässler, C., Heurich, M., & Brandl, R. (2009). Using airborne laser scanning to model potential abundance and assemblages of forest passerines. *Basic and Applied Ecology*, *10*, 671–681.

Müller, J., Stadler, J., & Brandl, R. (2010). Composition versus physiognomy of vegetation as predictors of bird assemblages: The role of lidar. *Remote Sensing of Environment*, *114*, 490–495.

Næsset, E. (2002). Predicting forest stand characteristics with airborne scanning laser using a practical two-stage procedure and field data. *Remote Sensing of Environment*, *80*, 88–99.

Næsset, E. (2004). Accuracy of forest inventory using airborne laser scanning: Evaluating the first Nordic full-scale operational project. *Scandinavian Journal of Forest Research*, *19*, 554–557.

Nelson, R., Keller, C., & Ratnaswamy, M. (2005). Locating and estimating the extent of Delmarva fox squirrel habitat using an airborne LiDAR profiler. *Remote Sensing of Environment*, *96*, 292–301.

Parresol, B. R. (1992). Baldcypress height-diameter equations and their prediction confidence intervals. *Canadian Journal of Forest Research*, *22*, 1429–1434.

Parresol, B. R. (2001). Additivity of nonlinear biomass equations. *Canadian Journal of Forest Research*, *31*, 865–878.

Patton, D. R. (1984). A model to evaluate Abert's squirrel habitat in uneven-aged ponderosa pine. *Wildlife Society Bulletin*, *12*, 408–414.

R Development Core Team (2012). *R: A language and environment for statistical computing.* Vienna, Austria: R Foundation for Statistical Computing.

Reutebuch, S. E., & McGaughey, R. J. (2012). *LIDAR-assisted inventory: 2012 Final report to Savannah River Site.* Report on file with USDA Forest Service-Savannah River, PO Box 700, New Ellenton, South Carolina 29809 (55 pp.).

Reynolds, R. T., Graham, R. T., Reiser, M. H., Bassett, R. L., Kennedy, P. L., Boyce, D. A., et al. (1992). *Management recommendations for the northern goshawk in the southwestern United States.* New Mexico, USA: USDA, Forest Service Southwest Region, Albuquerque.

Seavy, N. E., Viers, J. H., & Wood, J. K. (2009). Riparian bird response to vegetation structure: A multiscale analysis using LiDAR measurements of canopy height. *Ecological Applications*, *19*, 1848–1857.

Smart, L. S., Swenson, J. J., Christensen, N. L., & Sexton, J. O. (2012). Three-dimensional characterization of pine forest type and red-cockaded woodpecker habitat by small-footprint, discrete-return lidar. *Forest Ecology and Management*, *281*, 100–110.

Storch, I. (1995). Annual home ranges and spacing patterns of capercaillie in Central Europe. *Journal of Wildlife Management*, *59*, 392–400.

Tattoni, C., Rizzolli, F., & Pedrini, P. (2012). Can LiDAR data improve bird habitat suitability models? *Ecological Modelling*, *45*, 103–110.

Tweddale, S., Londo, H. A., Carney, J. M., Evans, D. L., Roberts, S. D., Parker, R. C., et al. (2008). In: R. A. Hill, J. Rosette, & J. Suarez (Eds.), *Proceedings of SilviLaser 2008: 8th International Conference on LiDAR applications in forest assessment and inventory* (pp. 586–595). Edinburgh, UK: Heriot-Watt University.

U.S. Fish and Wildlife Service (1970). United States list of endangered fish and wildlife. *Federal Register*, *35*, 16047.

U.S. Fish and Wildlife Service (2003). *Recovery plan for the red-cockaded woodpecker (Picoides borealis), second revision.* Southeast Region, Atlanta, Georgia, USA: U.S. Fish and Wildlife Service.

U.S. Fish and Wildlife Service (2011). *Revised recovery plan for the northern spotted owl (Strix occidentalis caurina).* Portland, Oregon, USA: U.S. Fish and Wildlife Service.

Valbuena, R., Mauro, F., Rodriguez-Solano, R., & Manzanera, J. A. (2010). Accuracy and precision of GPS receivers under forest canopies in a mountainous environment. *Spanish Journal of Agricultural Research*, *8*, 1047–1057.

Venables, W. N., & Ripley, B.D. (2002). *Modern Applied Statistics with S* (4th ed.). New York, New York, USA: Springer.
Vierling, K. T., Bässler, C., Brandl, R., Vierling, L. A., Weib, I., & Müller, J. (2011). Spinning a laser web: Predicting spider distributions using LiDAR. *Ecological Applications*, *21*, 577–588.
Vierling, K. T., Vierling, L. A., Gould, W. A., Martinuzzi, S., & Clawges, R. M. (2008). Lidar: Shedding new light on habitat characterization and modeling. *Frontiers in Ecology and the Environment*, *6*, 90–98.
Walters, J. R., Daniels, S. J., Carter, J. H., III, & Doerr, P. D. (2002). Defining quality of red-cockaded woodpecker foraging habitat based on habitat use and fitness. *The Journal of Wildlife Management*, *66*, 1064–1082.
Weakland, C. A., & Wood, P. B. (2005). Cerulean warbler (*Dendroica cerulea*) microhabitat and landscape-level habitat characteristics in southern West Virginia. *The Auk*, *122*, 497–508.
Williams, G. J. (2009). Rattle: A data mining GUI for R. *The R Journal*, *1*, 45–55.
Wulder, M.A., White, J. C., Nelson, R. F., Næsset, E., Ørka, H. O., Coops, N. C., et al. (2012). Lidar sampling for large-area forest characterization: A review. *Remote Sensing of Environment*, *121*, 196–209.
Zimble, D. A., Evans, D. L., Carlson, G. C., Parker, R. C., Grado, S.C., & Gerard, P. D. (2003). Characterizing vertical forest structure using small-footprint airborne LiDAR. *Remote Sensing of Environment*, *87*, 171–182.